Photonics applications III

✓ Optical nonlinearity in ChGs

Linear and nonlinear responses

❑ Linear optics regime

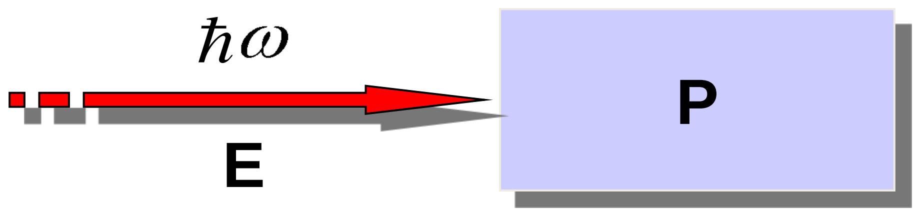

Effects: reflection, refraction, absorption, …

Material response:

$$\frac{\partial \mathbf{P}}{\partial \mathbf{E}} = \chi = \text{constant}$$

Superposition principle
➔ parallelism

❑ Nonlinear optics regime

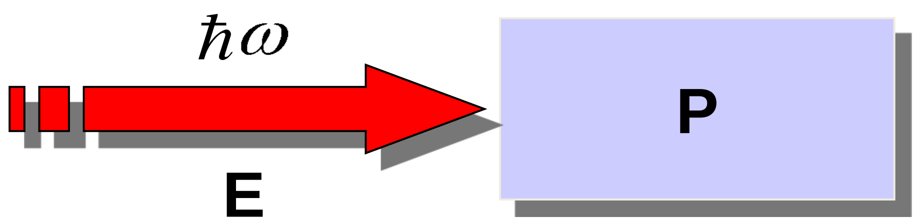

Effects: conversion, modulation, optical storage, …

Material response:

$$\frac{\partial \mathbf{P}}{\partial \mathbf{E}} = \chi(\mathbf{E}) \neq \text{constant}$$

Photon-matter-photon interaction

High-order optical susceptibility

- Electric field of monochromatic optical wave

$$\mathbf{E}(\mathbf{r},t) = \mathbf{A}(\mathbf{r},t)e^{i(\mathbf{k}\cdot\mathbf{r}-\omega t)} + c.c.$$

$$I(\mathbf{r},t) = 2c\varepsilon_0 n\left|\mathbf{A}(\mathbf{r},t)\right|^2 \quad \text{(SI)}$$

$$\mathbf{E}(\mathbf{r},t) = \frac{1}{2}\mathbf{A}(\mathbf{r},t)e^{i(\mathbf{k}\cdot\mathbf{r}-\omega t)} + c.c.$$

$$\mathbf{E}(\mathbf{r},t) = \mathbf{A}(\mathbf{r},t)\cos(\mathbf{k}\cdot\mathbf{r}-\omega t)$$

- Induced electric polarization

$$P_i = \varepsilon_0[\chi_{ij}^{(1)}E_j + \chi_{ijk}^{(2)}E_jE_k + \chi_{ijkl}^{(3)}E_jE_kE_l + \cdots] \quad \text{(SI)}$$

$$\chi_{ij_1\cdots j_n}^{(n)} = \frac{1}{\varepsilon_0 n!}\frac{\partial^n P_i}{\partial E_{j_1}\cdots\partial E_{j_n}}$$

$$P_i = \varepsilon_0\chi_{ij}^{(1)}E_j + \chi_{ijk}^{(2)}E_jE_k + \cdots \quad \text{(SI)}$$

$$P_i = \chi_{ij}^{(1)}E_j + \chi_{ijk}^{(2)}E_jE_k + \cdots \quad \text{(cgs)}$$

Nonresonant vs. resonant

- Nonresonant process
- (Near-)resonant process

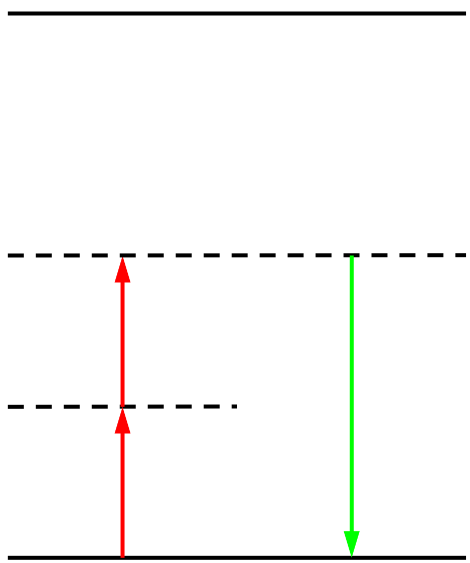

$$\mathrm{Re}(\chi_{NR}) < \mathrm{Re}(\chi_{R})$$

$$\mathrm{Im}(\chi_{NR}) < \mathrm{Im}(\chi_{R})$$

Resonance enhancement

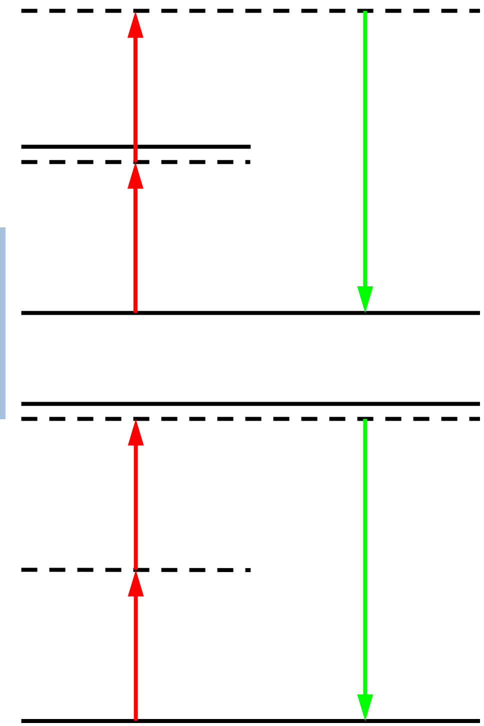

Instantaneous response

High nonlinearity, high loss

Conservation laws for photons in nonlinear optics

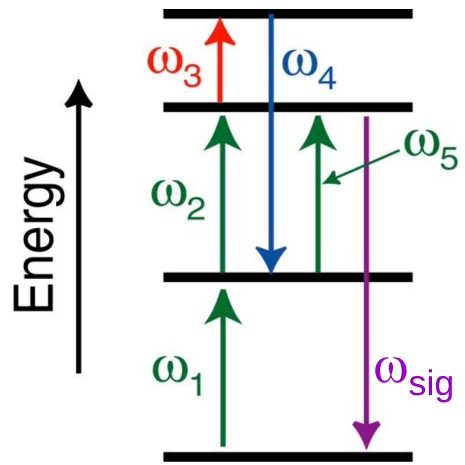

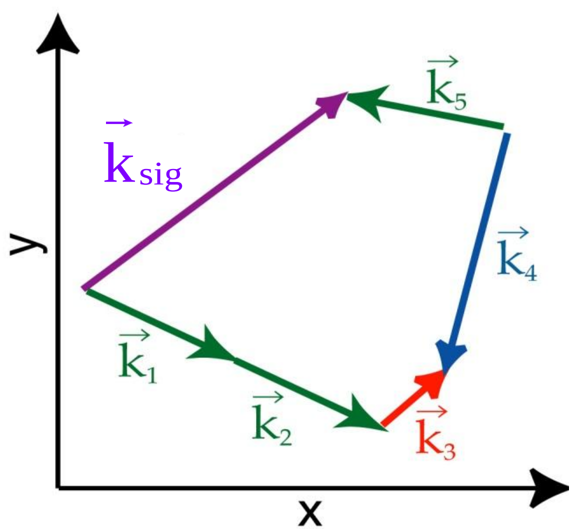

Energy conservation:

$$\omega_1 + \omega_2 + \omega_3 - \omega_4 + \omega_5 = \omega_{sig}$$

(The $\hbar$'s are canceled)

Momentum conservation:

$$\vec{k}_1 + \vec{k}_2 + \vec{k}_3 - \vec{k}_4 + \vec{k}_5 = \vec{k}_{sig}$$

Unfortunately, $\vec{k}_{sig}$ may not correspond to a light wave at frequency ω_{sig}!

Satisfying these two relations simultaneously is called "**phase-matching**."

Third-order optical susceptibility

- The lowest-order nonlinear effects in glasses originate from the third-order susceptibility $\chi^{(3)}$, which is responsible for THG, FWM and nonlinear refraction.

- Nonlinear refraction is the intensity dependence of the refractive index from the contribution of $\chi^{(3)}$, which leads to SPM, XPM…

✓ The refractive index of glass:

$$\overline{n}\left(\omega,\ |E|^2\right) = n(\omega) + n_2 |E|^2$$

$$n_2 = \frac{3}{8n} \chi^{(3)}_{xxxx}$$

Nonlinear effects and their applications

- ✓ Nonlinear refractive index;
  - ➢ Self-phase modulation (SPM)
  - ➢ Cross-phase modulation (CPM)
  - ➢ Four-wave mixing (FWM)
- ✓ Optical switch, wavelength conversion, super-continuum generation…
- ✓ Stimulated inelastic scattering;
  - ➢ Stimulated Raman Scattering (SRS)
  - ➢ Stimulated Brillouin Scattering (SBS)
- ✓ Amplifier or laser at IR wavelengths

Why ChG shows large optical nonlinearity?

- Miller's rule*;

$$\chi^{(3)} = \left(\chi^{(1)}\right)^4 10^{-10} \quad (esu)$$

- Boling's relation incorporating Abbe number**;

$$n_2 \propto \frac{n_0 - 1}{\nu^{\frac{5}{4}}}$$

- Chemical-bond relations in terms of covalency and polarity of atomic bonds**;

$$n_2 \propto \alpha_c^5 \left(3\alpha_p^2 - 1\right)$$

- Relationship for direct-gap semiconductors**;

$$n_2 = \frac{K' E_p^{1/2} G}{n_0^2 E_g^4}, \quad \beta = \frac{K' E_p^{1/2} F}{n_0^2 E_g^3}$$

* Ta'eed et al, Opt. Express, 15 (2007) 9205.

** Tanaka, J. Phys. Chem. Solids 68 (2007) 896.

Potential of ChG as a nonlinear optical material

- A broad transparent window from λ = 0.8~20 μm, and ultrahigh-speed third-order nonlinear response (< 100 fs) without carrier effects.
- A large nonlinear index simultaneously with relatively low TPA coefficient at λ ~1.55 μm.
- Fabricated at low temperature < 400°C, which is compatible to back-end process in Si-photonics.
- Photo-induced phenomena that can be used for the fabrication and post-tuning of devices.

Nonlinear optical properties

Table 1. Comparison of nonlinear optical properties of several third-order nonlinear materials at $\lambda = 1.5$ µm. [25, 58, 60]

Material	n_2 [$\times 10^{-20}$ m^2/W]	α_2 [10^{-12} m/W]	FOM
Chalcogenide glass (As_2S_3)	290	<0.01	>10
Chalcogenide glass (As_2Se_3)	1200	1	2
Bismuth Oxide (Bi_2O_3)*	110	-	-
Silicon (Si)	440	8.4	0.4
Silica (SiO_2)*	2.2	-	-

* The large optical band-gap of bismuth oxide and silica results in negligible two photon absorption at these wavelengths.

** FOM: nonlinear figure of merit incorporating TPA; $\dfrac{n_2}{\alpha_2 \lambda}$

Ta'eed et al, Opt. Express, 15 (2007) 9205.

Nonlinear optical properties

Table 1. *Figures of merit of various materials*

(Intensity (assumed) = 1 GW cm^{-2} → 100 W power. $W = n_2 I/\alpha_1 \lambda$ (goal: $W > 1$). $T = 2\lambda\alpha_2/n_2$ (goal: $T < 1$).)

material	n_2 /(cm^2 W^{-1})	α /cm^{-1}	W	λ /T	µm
semiconductors					
GaInAs (c.h.) ($\tau \sim 600$ fs)	4.5×10^{-12}	30–50	0.75	3	1.5
GaInAs (Kerr) ($\tau < 40$ fs)	-3×10^{-12}	30–50	0.5	4	1.5
AlGaAs (0.75 µm)	2×10^{-13}	0.1	8	< 0.3	1.56
organics					
PTS (crystal)	2.2×10^{-12}	< 0.8	> 10	< 0.1	1.60
DANS (polymer)	8×10^{-14}	< 0.2	> 5.0	≈ 0.2	1.32
glass					
SiO_2	2×10^{-16}	10^{-6}	$> 10^3$	$\ll 1$	> 1.06
RN (Corning)	1.3×10^{-14}	0.01	13	< 0.1	1.06
$As_{0.38}S_{0.62}$	4.2×10^{-14}	0.002	16	< 2	1.32

Stegeman and Torruellas, Phil. Trans. R. Soc. Lond. A 354 (1996) 745.

Nonlinear optical properties

Table 1. Linear and Nonlinear Optical Properties of the Measured Glasses

Glass	n_0 at 1.55 μm	λ_{gap} (μm)	λ = 1.25 μm: $n_2/n_{2,\text{fused silica}}$ (±15%)	λ = 1.25 μm: β (cm/GW) (±15%)	λ = 1.25 μm: FOM (±20%)	λ = 1.55 μm: $n_2/n_{2,\text{fused silica}}$ (±15%)	λ = 1.55 μm: β (cm/GW) (±15%)	λ = 1.55 μm: FOM (±20%)
$As_{40}S_{60}$	2.45	0.52	260	0.16	3	220	<0.030	>12
$As_{40}S_{50}Se_{10}$	2.49	0.55	400	0.14	6	380	0.16	4
$As_{40}S_{40}Se_{20}$	2.55	0.59	360	0.22	3	300	0.060	8
$As_{40}S_{30}Se_{30}$	2.62	0.62	580	0.38	3	430	0.15	5
$As_{40}S_{20}Se_{40}$	2.70	0.64	920	1.04	2	460	0.25	3
$As_{40}S_{10}Se_{50}$	2.76	0.67	1000	1.4	2	560	0.14	7
$As_{40}Se_{60}$	2.81	0.70	1200	2.8	1	930	0.14	11
$As_{39}Se_{61}$	2.81	0.70	–	–	–	660	0.28	4
$As_{40}Se_{55}Cu_5$	2.93	0.79	–	–	–	850	0.29	5
$As_{25}S_{55}Te_{20}$	2.52	0.79	–	–	–	470	0.15	5

Harbold et al, Opt. Lett. 27 (2002) 119.

Nonlinear optical properties; fiber

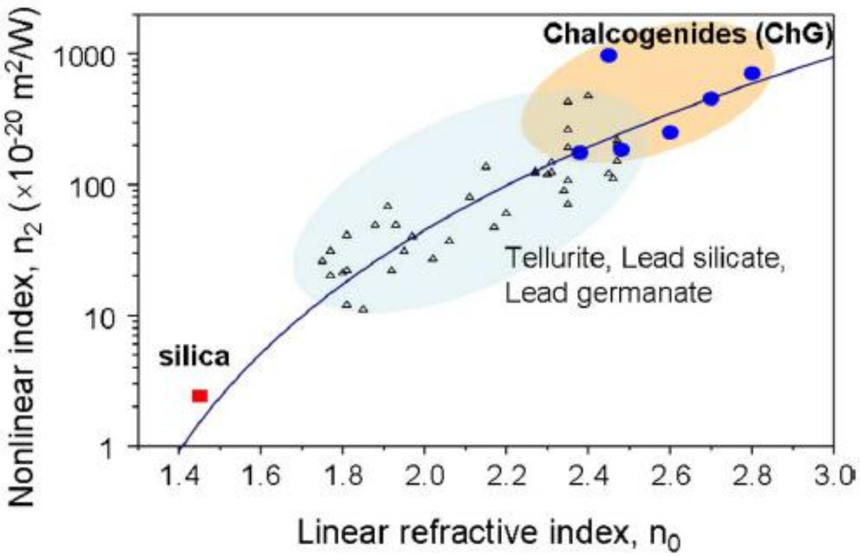

Fig. 1. (Curve) Miller's rule for nonlinearity index, n_2, versus refractive index, n_0, compared to measurements for (filled circles) various ChG glasses, (triangles) other highly nonlinear and (box) silica glasses, as in [28].

TABLE I
OPTICAL FIBER PARAMETERS AT 1550 NM

Parameter	Units	SiO_2 DSF	SiO_2 HNF	Bi_2O_3 fiber	As_2Se_3 fiber	As_2Se_3 taper
Nonlinear index (n_2)	n_2 of silica[a]	1	2.3	50	500	500
Effective core area (A_{eff})	μm^2	60	12	4	37	20
Nonlinearity coefficient (γ)	/W/km	1.9	17.5	1360	1200	2270
Dispersion (D)	ps/nm/km	-0.7	-0.1	-260	-560	-560

[a] n_2 of silica = $2.2\times10^{-20} m^2/W$ at 1550 nm.

Pelusi et al, IEEE J. Sel. Topics Quant. Electron. 14 (2008) 529.

Nonlinear absorption

Table 1
Physical and optical properties of several chalcogenide glasses

Composition	T_g (°C)	λgap (nm)	α_{1064} (cm^{-1})
As_2S_3	195	584	0.30
$GeSe_4$	160	737	0.34
$GeSe_6$	117	746	0.41
$(GeSe_4)_{1/2}(AsSe_3)_{1/2}$	133	750	0.30
As_2Se_3	185	809	0.61
$GeAs_2Se_2$	330	829	0.50
Pb-0	194	850	0.62
Pb-30	208	856	0.32

T_g: glass transition temperature; λgap: band-gap wavelength; α_{1064}: linear absorption coefficient at 1064 nm.

- Linear absorption of ChG?
- Nonlinear absorption of ChG?

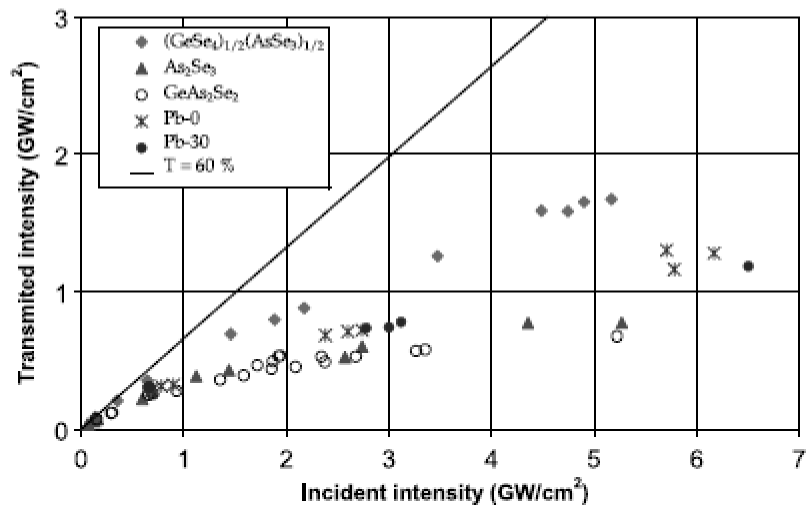

Fig. 2. Optical limiting behavior of $(GeSe_4)_{1/2}(AsSe_3)_{1/2}$ (◆), As_2Se_3 (▲), $GeAs_2Se_2$ (○) Pb-0 (✳) and Pb-30 (●). The sample thickness are respectively 1.18 mm, 1.44 mm, 1.26 mm, 1.88 mm and 0.94 mm.

Troles et al, Opt. Mater. 25 (2004) 231.

Nonlinear absorption

Table 2
Comparison of non-linear refractive index and two photons absorption coefficient between a Mach–Zehnder interferometer method and a *Z*-scan method for several chalcogenide glasses and CS_2 (use as reference)

	Mach–Zehnder interferometer [13,14]		*Z*-scan [10–12]	
	β (cm/GW)	$n_2 \times 10^{-18}$ (m^2/W)	β (cm/GW)	$n_2 \times 10^{-18}$ (m^2/W)
CS_2	0.0	3.1	0.0	3
As_2S_3	0.08	5.0	0.1	4.5
$GeSe_4$	1.8	8.3	1.7	13
$GeSe_6$	1.7	11.5	1.5	17
$(GeSe_4)_{1/2}(AsSe_3)_{1/2}$	2.5	12	2.7	22
As_2Se_3	4.4	19	4.5	18
$GeAs_2Se_2$	5.4	10	5.9	18.5
Pb-0	2.8	8	–	–
Pb-30	5.7	14	–	–

β: two photon absorption coefficient; n_2: non-linear refractive index.

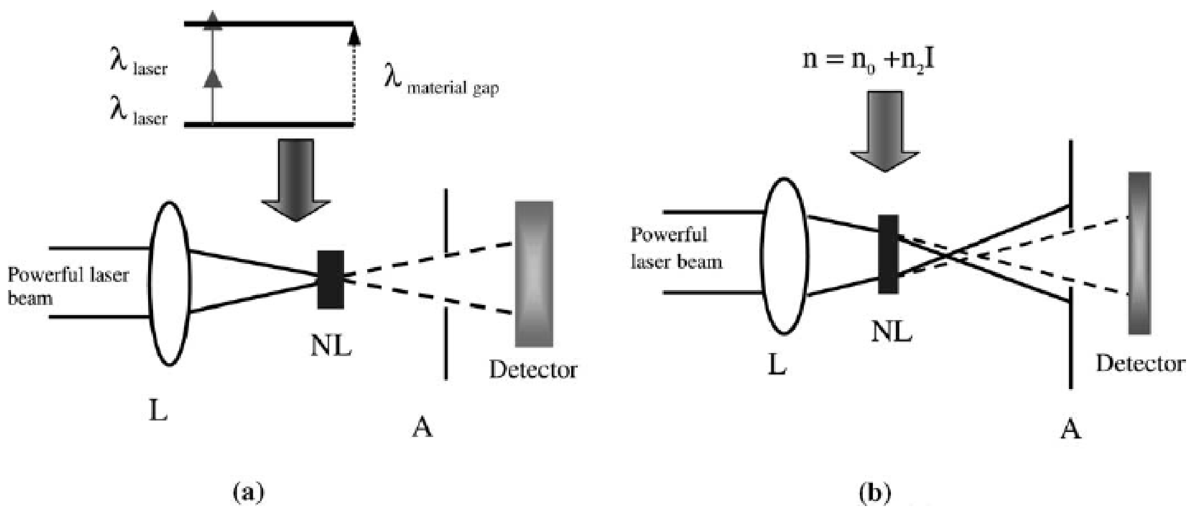

Fig. 3. Optical limiters based on third order non-linear optical properties: (a) two photons absorption, (b) non-linear refraction. L: lens, NL: non-linear material, A: aperture.

Troles et al, Opt. Mater. 25 (2004) 231.

Nonlinear absorption

Chalcogenide glasses present high values for third-order non-linear optical properties, i.e., high non-linear refractive indices (800 times as high as the non-linearity of silica glass at 1.064 μm) and a high non-linear absorption coefficient, which can reach more than 5 cm/GW. We study here the optical limiting properties of several chalcogenide glasses at 1.064 μm with a picosecond pulsed Nd:YAG laser and we observed a real optical limiting behavior. In the case of $GeAs_2Se_2$, glass for example, the decrease of the transmitted intensity is around 75% compared to the theoretical linear transmission, for incident pulses of 5 GW/cm^2. The comparison between the theoretical non-linear transmission induced by the two photon absorption effect and the experimental non-linear transmittance shows that the optical limiting properties are mainly due to non-linear absorption.

- ✓ Linear absorption of ChG?
  - ➢ Weak absorption tail; processing dependent
- ✓ Nonlinear absorption of ChG?
  - ➢ Bandgap energy; composition dependent

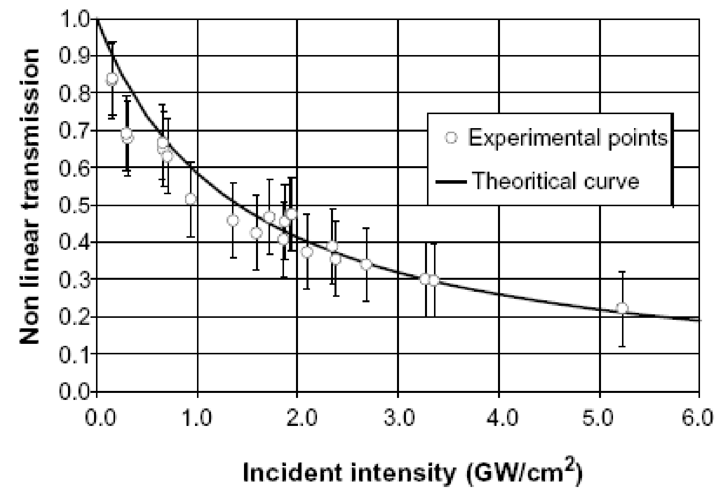

Fig. 4. Theoretical non-linear transmittance and experimental points for: $GeAs_2Se_2$, 1.26 mm sample thickness and $\beta = 5.4$ cm/GW.

Troles et al, Opt. Mater. 25 (2004) 231.

Experimental demonstrations

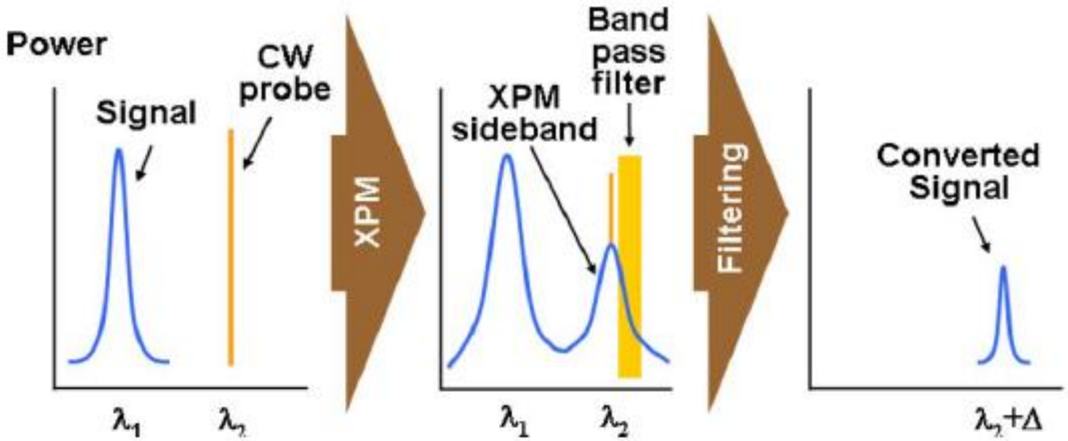

Fig. 3. Principle of wavelength conversion by XPM and optical filtering.

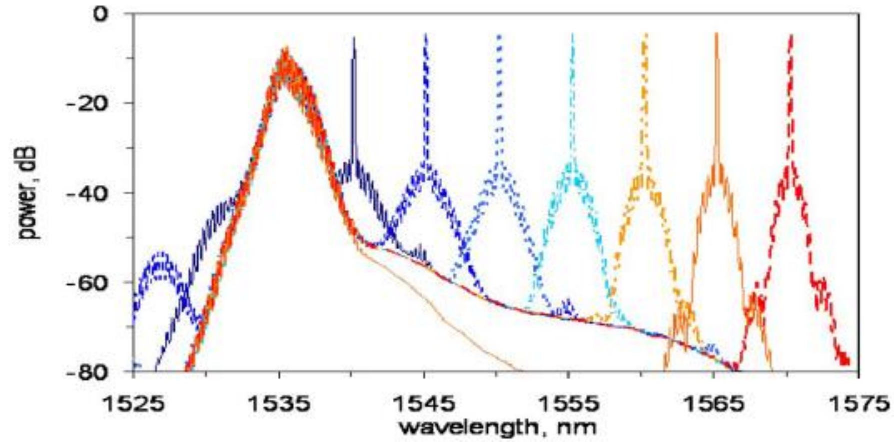

Fig. 5. Overlaid output optical spectra from a 16-cm length As_2Se_3 fiber taper for different CW wavelengths with 40 Gb/s signal fixed at 1535 nm.

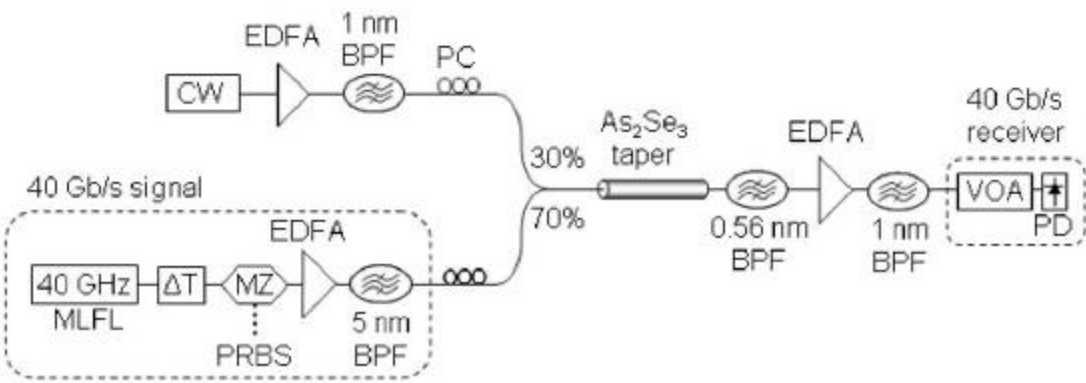

Fig. 4. Experimental setup for 40-Gb/s wavelength conversion in a 16-cm length tapered As_2Se_3 fiber.

TABLE II
CHALCOGENIDE WAVEGUIDE COMPARISON

Parameter	Units	As_2Se_3 taper	As_2S_3 rib (2.7×3.8 μm)	As_2S_3 rib (2.6×4 μm)
Length (L)	cm	16	5	22.5
Insertion Loss	dB	5	7.5	6.5
Refractive Index (n)	-	2.8	2.37	2.37
Nonlinear index (n_2)[a]	n_2 of silica	500	132	132
Effective core area (A_{eff})	μm^2	20	5.7	7.1
Nonlinearity coefficient (γ)[†]	$W^{-1}\ km^{-1}$	2270	2080	1700
Dispersion (D)[†]	ps/nm/km	-560	-286	-342

[a] n_2 of silica = $2.2\times10^{-20} m^2/W$ at 1550 nm wavelength
[†] at 1550 nm wavelength

Pelusi et al, IEEE J. Sel. Topics Quant. Electron. 14 (2008) 529.

Experimental demonstrations

- Wavelength conversion, via FWM, of a 40 Gb/s signal over 40 nm.
- All-optical demultiplexing of a 160 Gb/s signal down to 10 Gb/s.

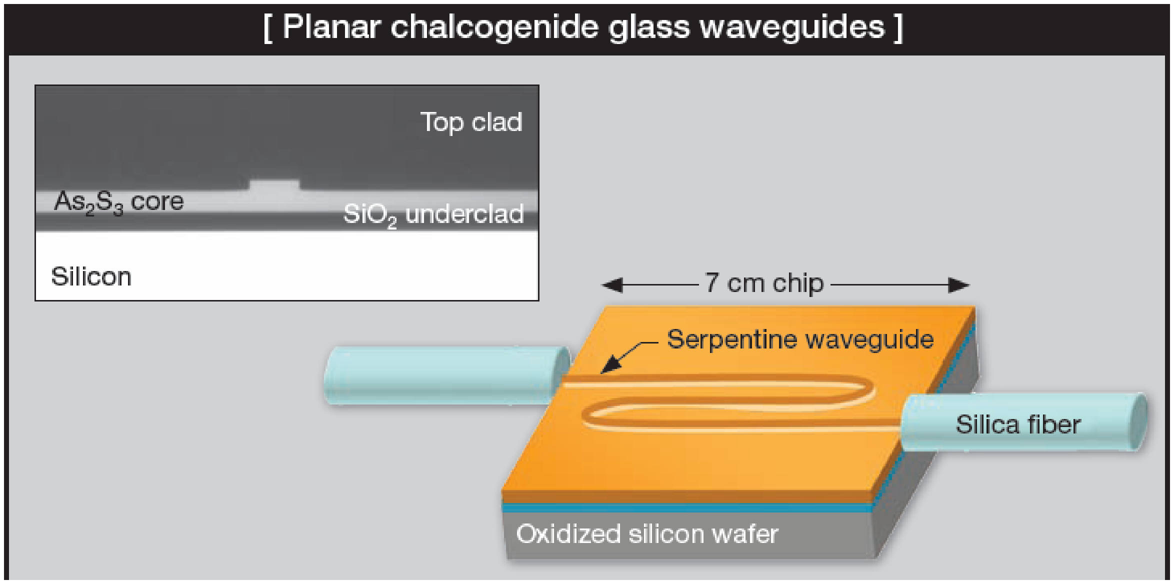

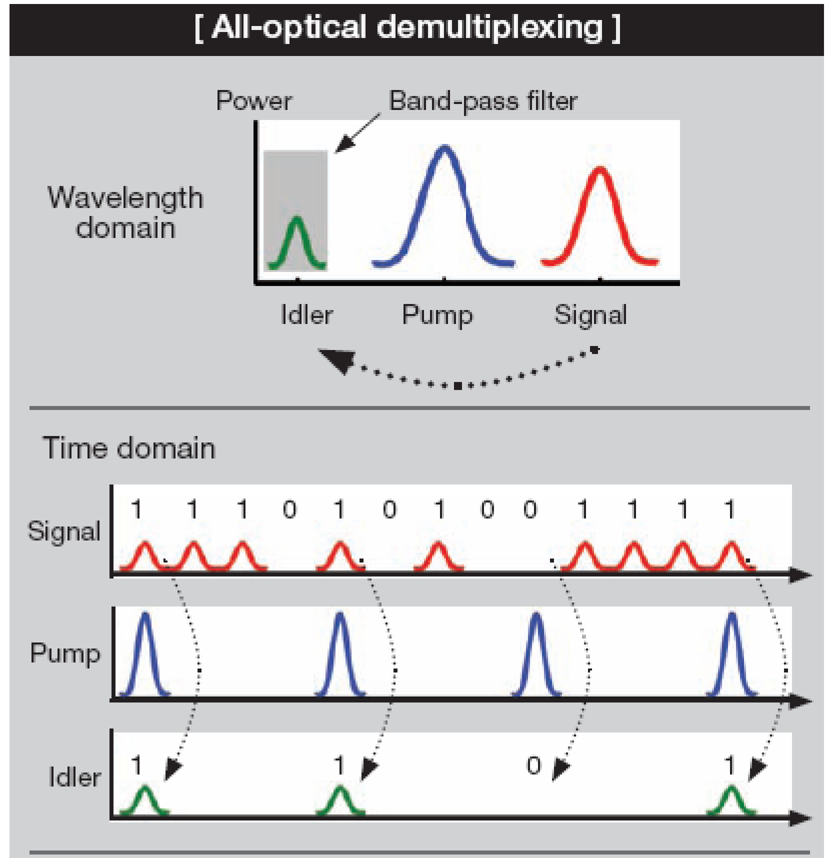

Ta'eed et al, IEEE Photon. Technol. Lett. 19 (2006) 1496.

Super-continuum generation

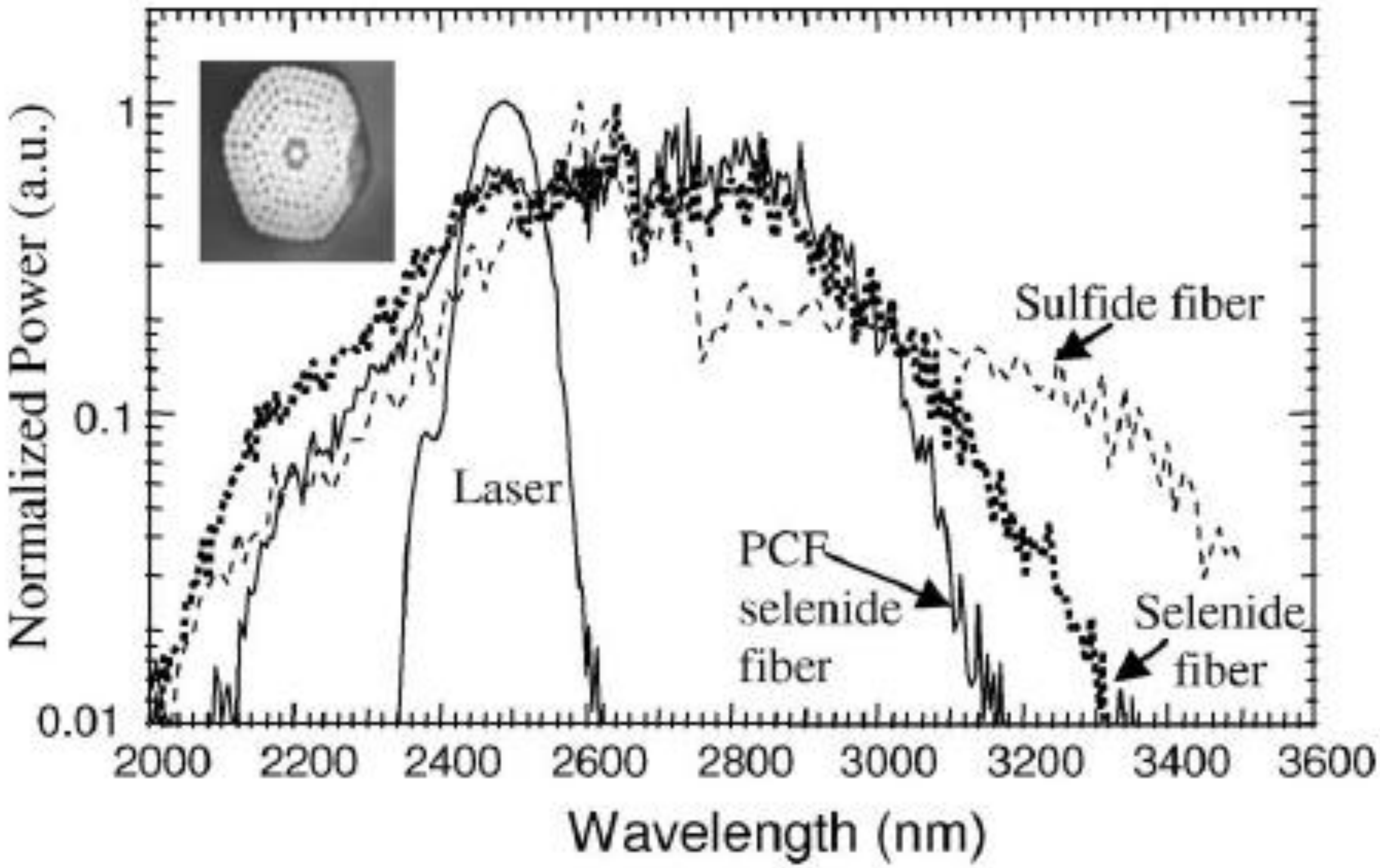

Fig. 9. Supercontinuum generation in small-core chalcogenide fibers. The insert shows the cross-sectional view of the selenide PCF fiber.

Sanghera et al, IEEE J. SELECTED TOPICS IN QUANTUM ELECTRONICS 15 (2009) 114..

SBS and SRS

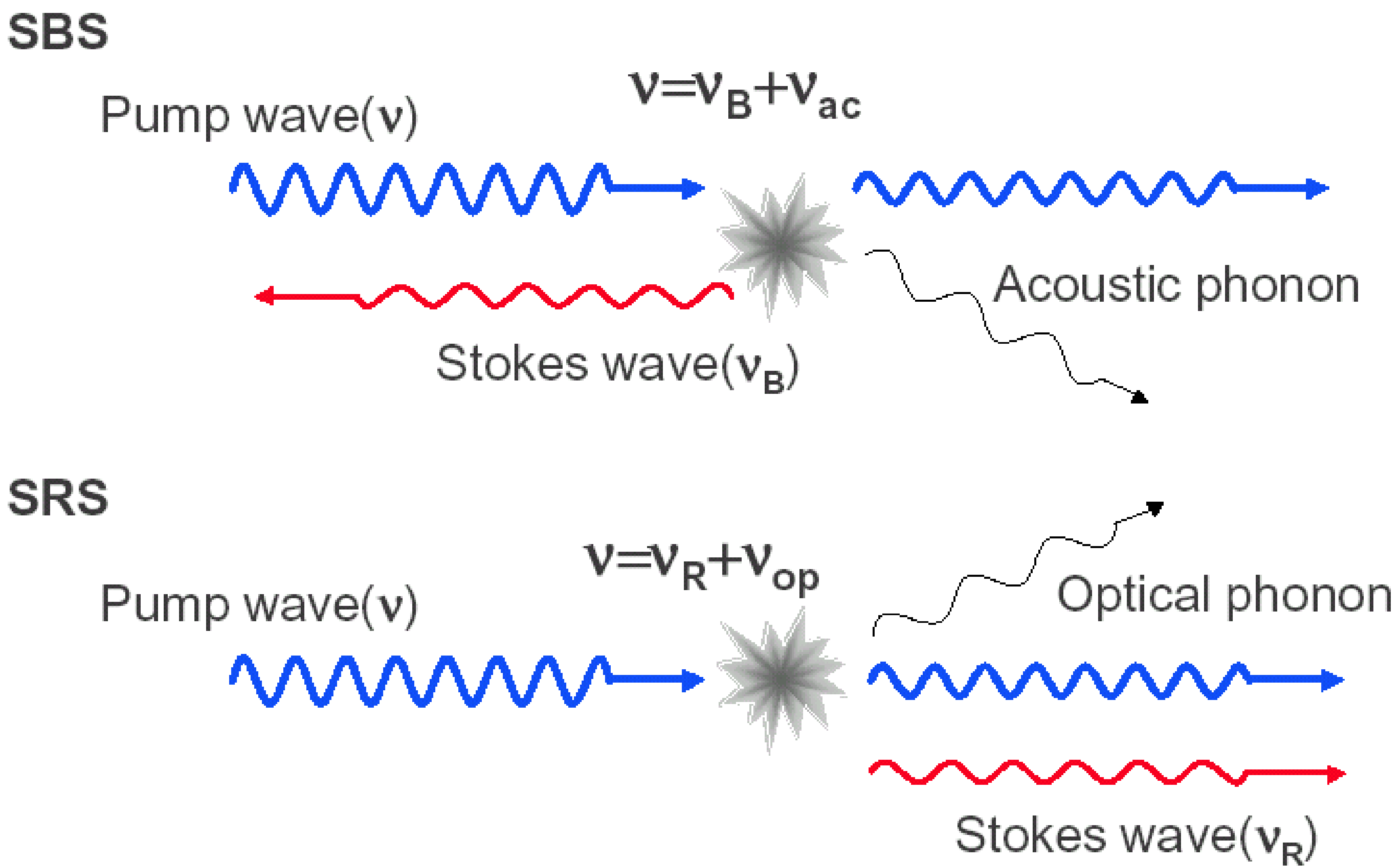
SBS
Pump wave(ν)
ν=ν_B+ν_ac
Stokes wave(ν_B)
Acoustic phonon
SRS
Pump wave(ν)
ν=ν_R+ν_op
Optical phonon
Stokes wave(ν_R)

Raman shift

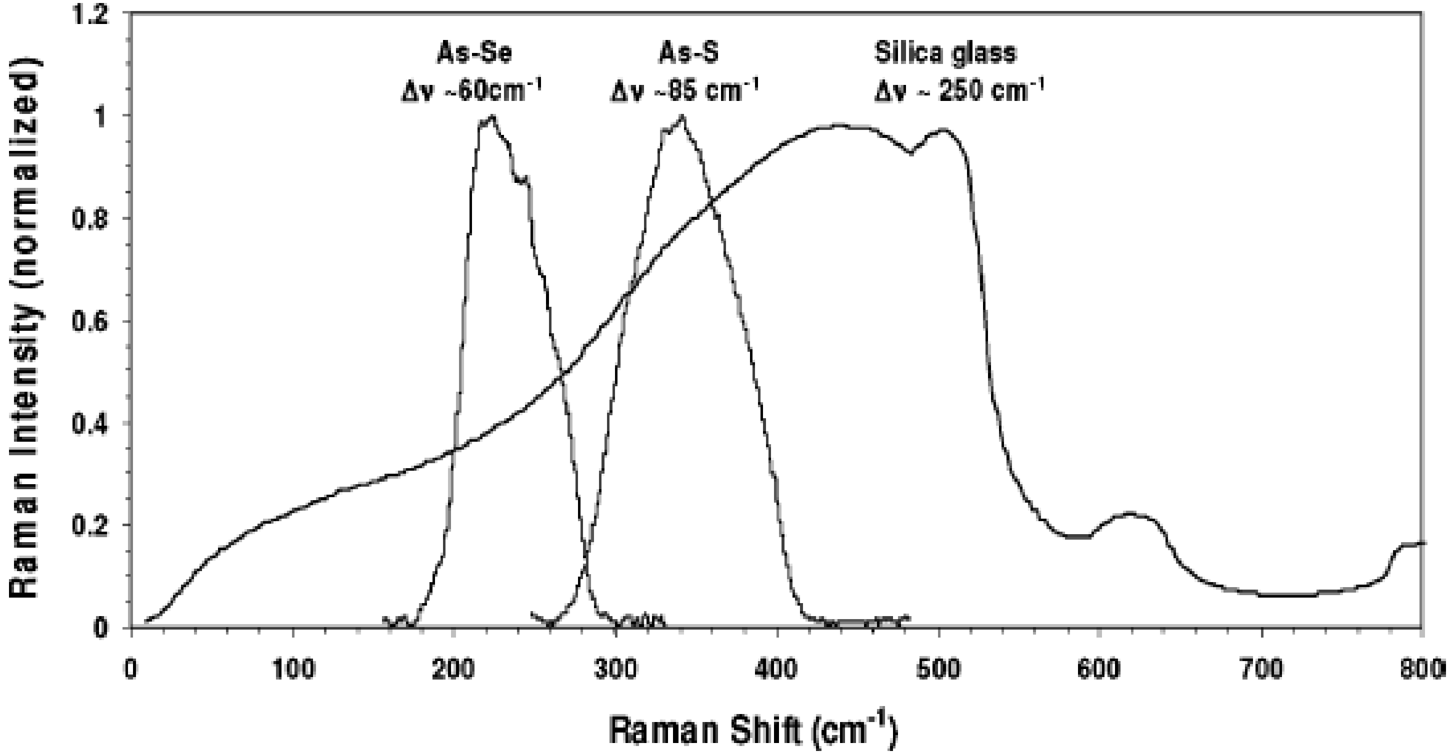

Fig. 6. Raman spectra of As_2S_3 and As_2Se_3 glass. Silica glass is shown for reference.

Sanghera et al, IEEE J. SELECTED TOPICS IN QUANTUM ELECTRONICS 15 (2009) 114..

Stimulated Raman scattering

TABLE II
FIGURE OF MERIT FOR RAMAN AMPLIFICATION IN As–Se FIBER AT 4-μm-COMPARED RAMAN AMPLIFICATION IN SILICA FIBER AT 1.5 μm

	λ (µm)	g_R (cm/W)	Loss (dB/km)	α (cm^{-1})	FOM ($10^{-6}W^{-1}$)
Silica Fiber	1.5	0.65 x 10^{-12}	0.2-0.3	~6 x 10^{-7}	1.1
As-Se Fiber	4	1.7 x 10^{-10}	200	5 x 10^{-4}	0.34
			3	7.5 x 10^{-6}	23

The loss value of 200 dB/km (a) for As–Se is typical of a "champion" loss value. The loss value of 3 dB/km (b) is theorecial loss.

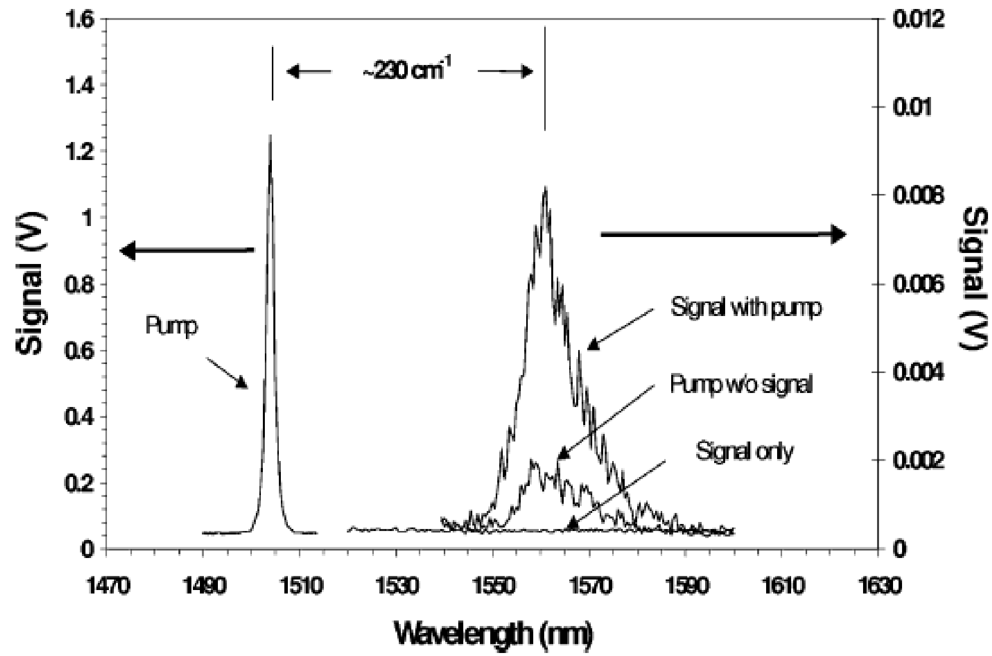

Fig. 7. Raman amplification in As–Se fiber. Shown is the amplifier output with signal and no pump, pump and no signal (showing background stimulated Raman scattering (SRS) resulting from pump), and amplified signal with pump.

Sanghera et al, IEEE J. SELECTED TOPICS IN QUANTUM ELECTRONICS 15 (2009) 114..

Stimulated Raman scattering

Table 1. Peak Raman gain coefficients of the measured germanium and arsenic based chalcogenide glasses, ratio of $n_2/n_{2,silica}$, and the surface optical damage threshold at 1064 nm using 25 ps pulse durations.

Glass Composition	$g_{RG} \times 10^{-13}$ (m/W) @ Δυ (THz) [Ref]	$n_2/n_{2,\ silica}$ [Ref]	1064 nm surface optical damage threshold (GW/cm^2)
$Ge_{23}Sb_7S_{70}$	71 ± 7 @ 10*	55 [8]	7.2
$Ge_{18}Ga_5Sb_7S_{70}$	65 ± 4 @ 10*	65 [8]	6.3
$Ge_{18}Ga_5Sb_7S_{68}Se_2$	68 ± 7 @ 10*	53 [11]	6.0
$Ge_{18}Ga_5Sb_7S_{65}Se_5$	72 ± 10 @ 10*	63 [11]	5.4
As_2S_3	74 ± 15 @ 10*	73** [13]	8.4
$As_{24}S_{38}Se_{38}$	155 ± 11 @ 7.8*	406** [13]	3.5
$50TeO_2–50Tl_2O$	52 ± 3 @ 21.3 [12]	33 [15]	5.1
SiO_2	0.9 ± 0.2 @ 13.2 [9]	1	< 100

* this work ** measured at 1.6 μm [13]

R. Stegeman et al, Opt. Express 14 (2006) 11702.

ChG Raman laser; a simulation

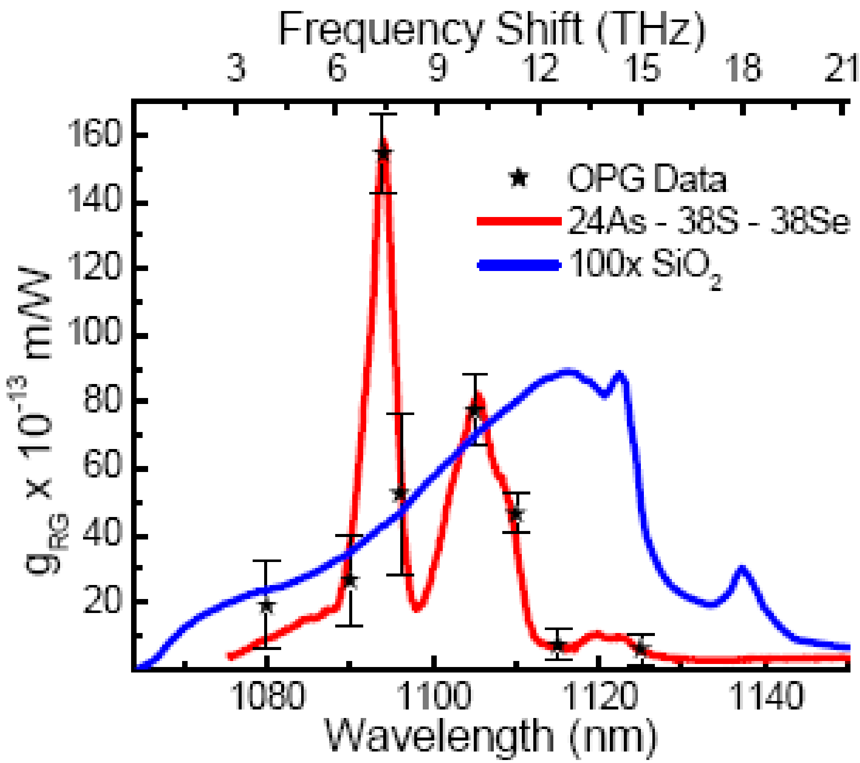

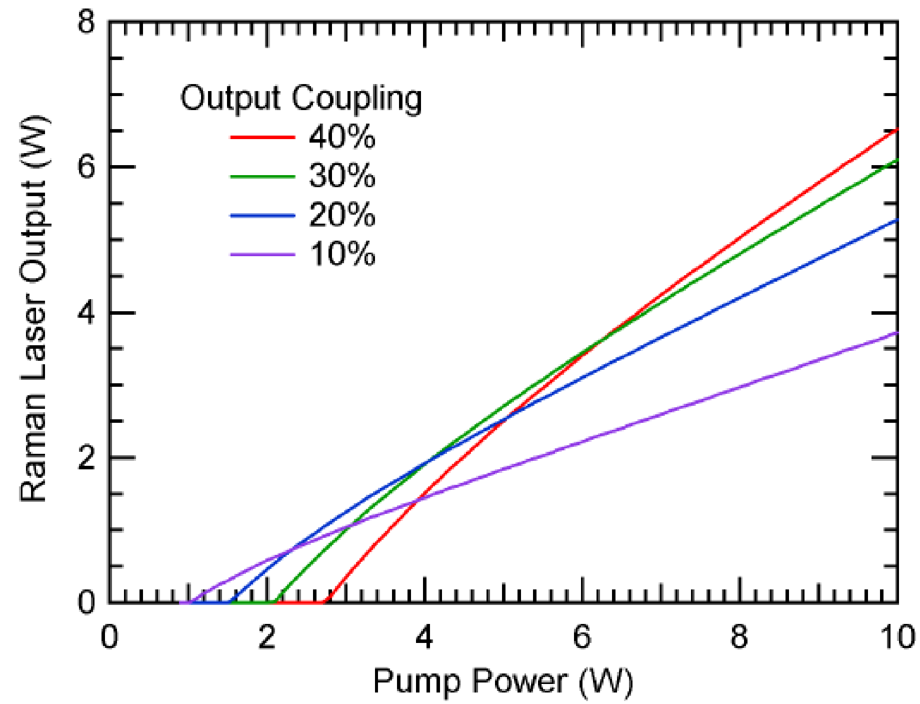

Left figure: Stegeman et al, Opt. Express 14 (2006) 11702.
Right figure: Thielen et al, Opt. Express 11 (2003) 3248.

Stimulated Brillouin scattering

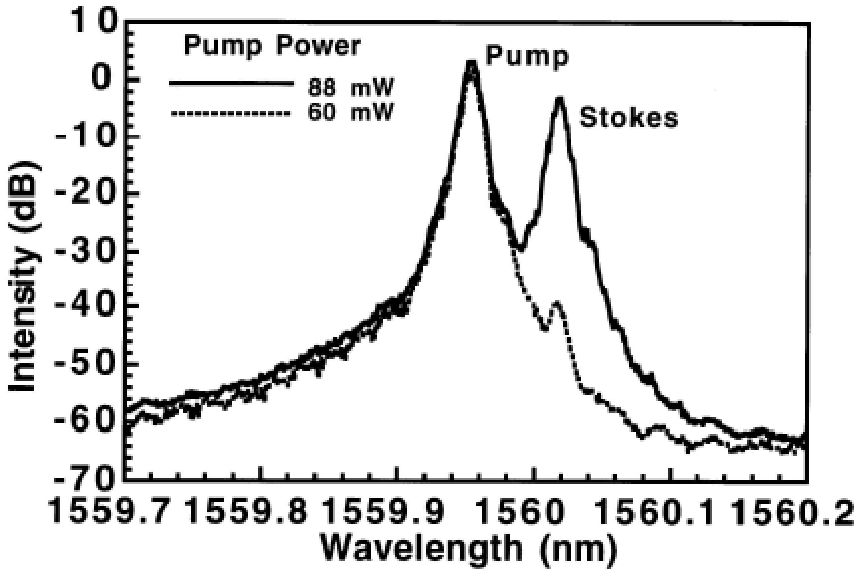

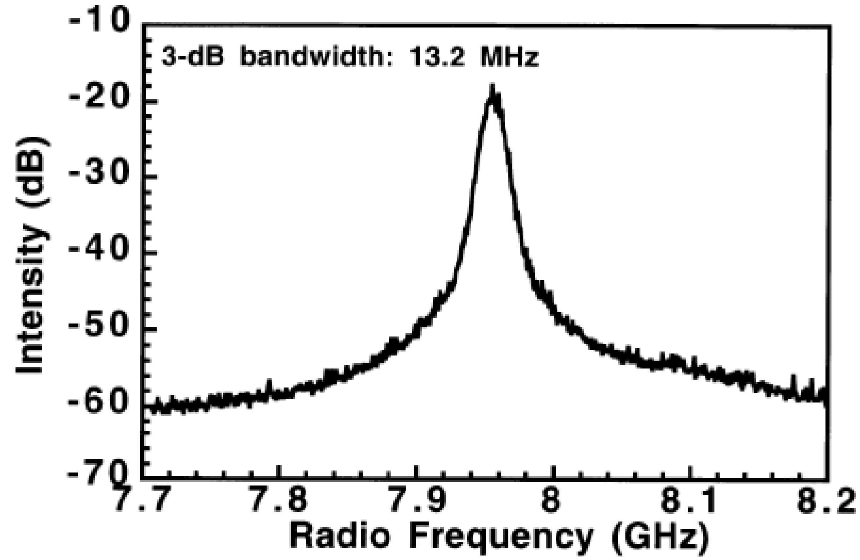

Table 1. Brillouin shift, linewidth and gain coefficients of As_2Se_3 and fused silica at 1.56 μm

Material	n	ρ (kg/m^3)	v_A (m/s)	p_{12}	$\Delta\nu_B$ (MHz)	ν_B (GHz)	g_B (m/W)
As_2Se_3	2.808[a]	4640[b]	2250[b]	0.266[c]	13.2[d]	7.95[d]	6.08×10^{-9}
Fused silica	1.45	2200[b]	5960[b]	0.286[e]	16[f]	11.1[g]	4.52×10^{-11}

Abedin, Opt. Express 13 (2005) 10266.

Acousto-optic effect

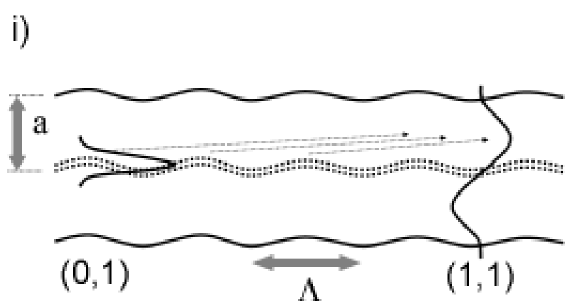

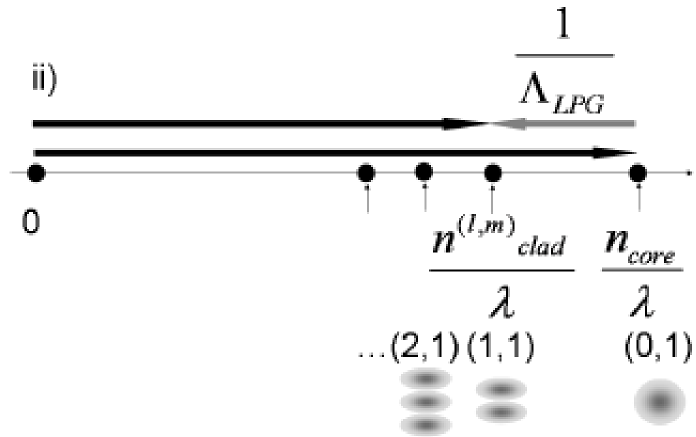

$$\lambda_{LPG} = \Lambda(n_{core} - n^{(l,m)}_{clad})$$

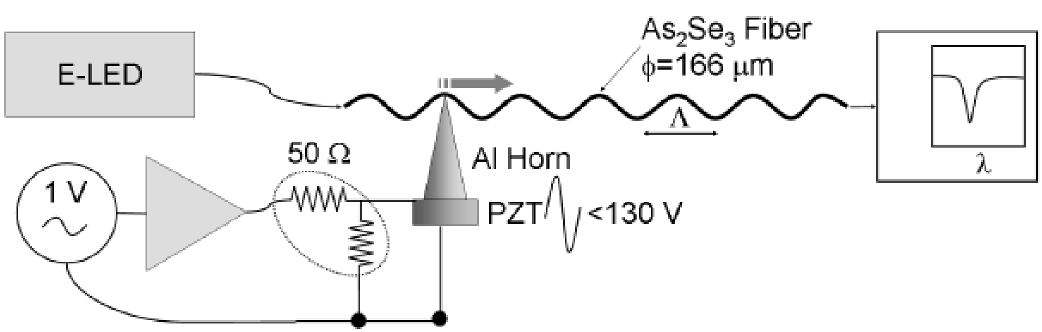

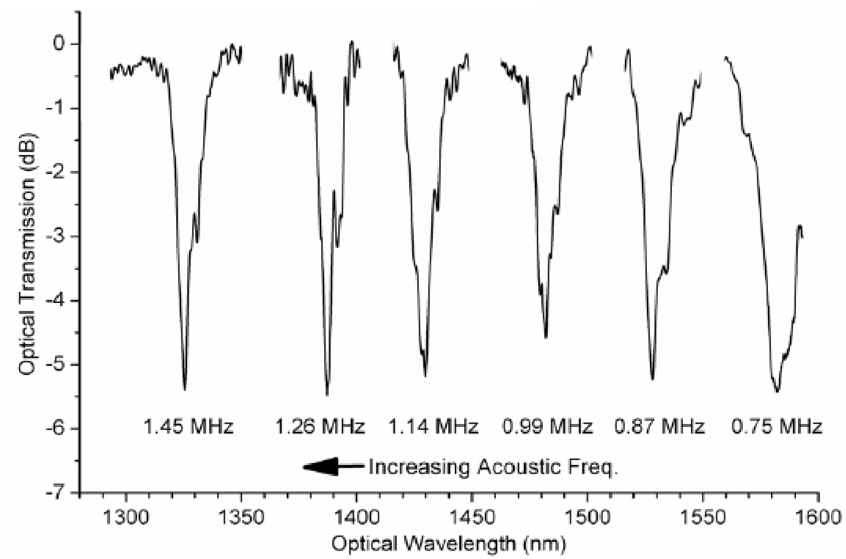

Littler et al, Opt. Express 14 (2006) 8088.

Second harmonic generation

- ✓ Photo-induced SHG (optical poling) in 20Ge-20As-60S glass*
  - ➢ A nanosecond pulsed Nd: YAG laser were used.
  - ➢ A 10^4 larger SHG magnitude than $15Nb_2O_5$-$85TeO_2$ glass.
  - ➢ The large and stable value of $\chi^{(2)}$ attributed to the induced defect structures and large $\chi^{(3)}$ of the ChG.

- ✓ Thermal poling of 5Ga-20Ge-10Sb-65S glass**
  - ➢ A reproducible $\chi^{(2)}$ susceptibility of 4.4 ± 0.4 pm/V achieved for specific poling conditions.
  - ➢ Accumulation of negative charges near the anodic side creating a high electric field.

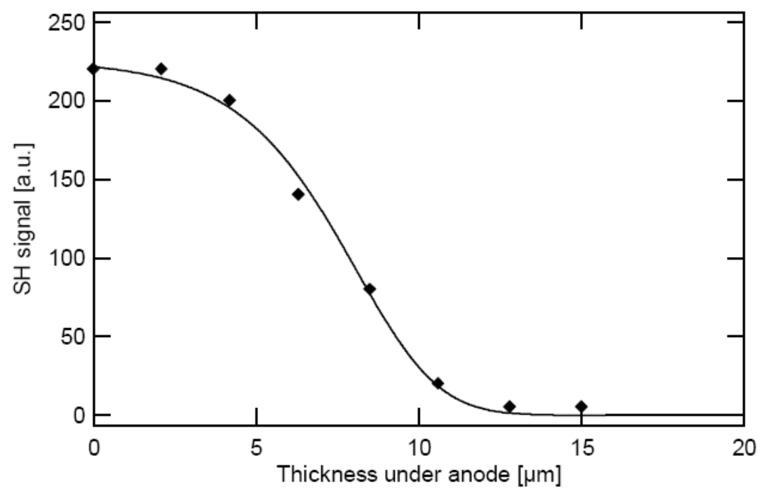

Fig. 3. Remaining SH signal after successive etching operations. The filled dots represent experimental points. The black line represents the best theoretical fit.

*Qiu et al, Opt. Lett. 26 (2001) 914.

**Guignard et al, Opt. Express 13 (2005) 789.